[16] *Dave, A., U. Vaishnav, R. Desai, A. Shah, B. Ankleshwaria,* and *M. Mehta:* On the assessment of hydrogels for fluid absorbency. J. Appl. Polym. Sci. **58** (1995), 853–859.
[17] *Abdul-Razik, E. A.:* Homogeneous graft copolymerization of acrylamide onto ethyl cellulose. Polymer **31** (1990), 1739–1744.
[18] *Stout, E. I., D. Trimnell, W. M. Doane,* and *C. R. Russell:* Graft copolymers of starch-polyacrylonitrile prepared by ferrous ion-hydrogen peroxide initiation. J. Appl. Polym. Sci. **21** (1977), 2565–2573.

Address of authors: *Dr. *Vilas D. Athwale,* M. Sc., Ph. D., Reader in Physical Chemistry, Department of Chemistry.

Mrs. *Vidyagauri V. Lele,* M. Sc., M. Phil., Department of Chemistry, University of Mumbai. Vidyanagari, Mumbai-400 098.

* Author to whom all correspondence should be addressed.

(Received: May 30, 1998).

Characterization of Acetyl Starch by Means of NMR Spectroscopy and SEC/MALLS in Comparison with Hydroxyethyl Starch

Dorothee Heins, Werner-Michael Kulicke, Peter Käuper and Heiko Thielking, Hamburg (Germany)

The properties of starch derivatives which may be used as plasma substitutes, are dependent upon the molecular structure. Seven acetyl starch (AS) samples were determined and compared with results from hydroxyethyl starch (HES) samples.
The molar masses and their distributions were determined with the combination of size exclusion chromatography and light scattering. Slightly asymmetric distributions were determined with a polydispersity $M_w/M_n \cong 2.4$ and weight-average molar masses of M_w = 250,000–300,000 g/mol for six AS samples and $M_w/M_n \cong 3.6$ and a weight-average molar mass of 766,000 g/mol for one AS sample.
The average degrees of substitution (DS) and the substitution pattern were determined by high resolution NMR spectroscopy. The AS samples investigated had a DS of 0.42 to 0.81, comparable to HES, but the regioselective substitution pattern revealed differences. While for HES the position C-2 is preferred and the position C-3 has nearly no substituent, for AS both positions, C-2 and C-3, are substituted likewise.
Degradability by α-amylase was tested in the laboratory for AS as well as for HES having nearly the same degree of substitution and molar mass, but C-2/C-6 = 2 for AS and C-2/C-6 = 1.4 for HES. An exponential decrease in the molar mass was observed over time, down to a limiting molar mass $M_w \cong 50{,}000$ g/mol for AS and $M_w \cong 30{,}000$ g/mol for HES, the degradation of AS occurred more slowly.

1 Introduction

Colloidal plasma substitutes are aqueous solutions of colloids and electrolytes isotonic with blood, which are used to replace lost blood. They stabilise the circulation, dilute the blood (haemodilution) and improve the microcirculation.

The best way to replace a lost volume of blood still involves supplying stored blood. However, there is a continuously growing market for man-made colloidal plasma substitutes because they exclude the risk of disease being transmitted and ensure sterility of the product. The polymer solutions have a long shelf life, are easy to store, are available in any quantity and are cheap to produce [1].

Plasma substitutes need to have the same colloid-osmotic pressure as the original blood plasma. Therefore, polymeric substances such as polyvinylpyrrolidone, gelatine, dextran or hydroxyethyl starch have been or still are used. As a function of the concentration, these substances are not only able to make up the lost volume, but also increase the osmotic pressure and make interstitial water move into the bloodstream. These are the so called plasma volume expanders [2].

Today hydroxyethyl starch (HES) is one of the most commonly used plasma substitutes: in 1996 its share of the German market was 81 %, that of gelatine 17 % and dextran 2 % [3]. Polyvinylpyrrolidone is no longer used because it accumulates in the human body [2]. But even a highly developed product such as HES can result in anaphylactoid reactions, and also has persistent fractions which accumulate in the reticulo-endothelial system [1]. In addition it has been reported that HES may cause a long-lasting itching, which is resistant to therapy. Other side-effects of HES may include influences on the function of the kidneys and on blood clotting [1, 4].

In recent years a lot of research has been aimed at correlating the molecular structure of HES with the unwanted side-effects. It has been shown that the degree of substitution by hydroxyethyl groups, especially their distribution over the various different positions, has a significant effect on the retention time in the human body. Substitution at position C-2 means that cleavage of the α-glycosidic bond by α-amylase is subject to strong steric hindrance, whereas this effect is only weak when substitution is at position C-6 [5].

The molar mass and molar mass distributions were determined for laboratory and commercial products. The results showed very different distributions with respect to the high molar mass tail. For instance, a commercially available HES sample with a mean molar mass of 40,000 g/mol had molar masses up to several million g/mol [6]. The high molar mass tail is said to be responsible for side-effects such as anaphylactoid reactions.

Recent research activities have looked at acetyl starch as a substitute for common HES products [7]. Since starch is retained as the starting material, the products are expected to

  0038-9056/98/1010-0431$17.50+.50/0

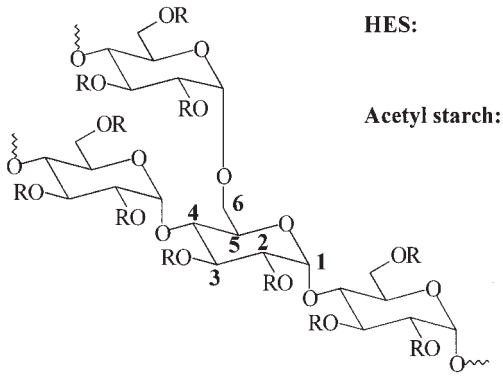

Fig. 1. Schematic representation of a section from the chain of the starch derivatives.

have comparable colloid-osmotic properties. Taking the acetyl group as a substituent should lead to a more homogeneous functionalization because a second substitution at the same atom is ruled out (see formula in Figure 1, n > 1 in the formula of HES indicates multiple substitution).

In addition, it has been reported that degradation of HES is slow and incomplete because etherification hinders the attack of the α-amylase [7]. Prolonged application of HES may lead to accumulation in the human body which is said to be responsible for long-lasting itching. Changing the ether bond to an ester bond increases the biological degradability of the polymeric backbone because the ester bond, which would otherwise hinder the attack of the α-amylase, is split by esterases [7].

A set of these novel products is investigated by methods of polymer analysis. The parameters of interest include the chemical and solution structures as determined by the degree of substitution, the substitution pattern, molar mass distributions and root mean square radii. The aim is to gain a first impression of the expected properties, based on the known structure-property-relationships for common HES products. Furthermore, interest also focuses on whether the enzymatic degradation of the acetyl group has different kinetics to that of HES.

2 Experimental Section

^{13}C NMR spectroscopy

The {^{1}H}-^{13}C NMR spectra were recorded by means of a MSL 300 spectrometer (Bruker, Germany) with a 10 mm probehead. Deuterium oxide solutions, 10 % with respect to the polymer, were used. To enable the proton decoupled spectra to be quantitatively evaluated, the inverse gated decoupling technique (IGATED) for complete suppression of the nuclear *Overhauser* effect (nOe) was applied. The spectra were recorded at room temperature with a minimum of 2,500 scans. The operating parameters were as follows: frequency 75.47 MHz, sweep width 17.2 kHz, relaxation delay 10 s, pulse angle 60 degrees, reference trimethylsilylpropionic acid-d_4 sodium salt (δ = –2.78 ppm). Quantitative evaluation of the spectra was carried out by fitting a set of Lorentzian lines to the spectra with the aid of the Bruker software WinNMR on a PC.

SEC/MALLS

A schematic diagram of the system used in this study can be found in ref [6]. Four TSK-columns (Toso Haas, Stuttgart, Germany) with decreasing exclusion limit were coupled to a DAWN-F light scattering photometer (Wyatt Technology Corp., Santa Barbara, CA, USA) and from there the eluent was routed into a differential refractive index detector (DRI) Shodex RI SE-51 (Showa Denko, Tokyo, Japan). The carrier solution was deionized, double distilled water containing 0.1 M sodium nitrate or sodium acetate/acetic acid was used as a polyelectrolyte and 0.02 % (w/w) of sodium azide as a bactericide. The solutions were purified by filtration (0.1 μm) and degassed on-line (Knauer, Bad Homburg, Germany). The samples were dissolved in the carrier solution overnight without stirring. The injection volumes were 100 μL and 250 μL with an amount of 0.002 mg and 0.05 mg for each sample. The DAWN-F was calibrated with ultrapure toluene and eighteen fixed scattering angles were normalized with a dispersed solution of gold having a known diameter. The "spider" plot method [8] was used for determination of the interdetector volume. The signal of the DRI detector was routed to the DAWN-F, which was interfaced to an AT computer.

Refractive index increment

All samples were measured in acetate buffer and no evidence was found of the refractive index increment being dependent upon molar mass (as known from other polymer solvent systems). The measurements were performed with a Wood RF-600 (Wood Co., PA, USA) and a Shodex RI SE-51 (Showa Denko K.K., Tokyo, Japan). On the basis of the above results only two samples were measured in sodium nitrate to obtain the corresponding refractive index increment.

Materials

The acetyl starches investigated were a set of samples with differing degrees of substitution. Apart from sample AS/e 7 which had a nominal molar mass of 400,000 g/mol, all the remaining samples had a nominal molar mass of 200,000 g/mol. The hydroxyethyl starch sample had a nominal molar mass of 200,000 g/mol. All acetyl starch samples are abbreviated to AS, and the hydroxyethyl starch sample to HES. During synthesis natural starch has to be degraded to obtain the appropriate molar mass range. Some of the samples were degraded by acid (indicated by an "a" after the letters) instead of the usual enzymatic process (indicated by an "e"). The moisture content of the samples was measured thermogravimetrically.

Enzymatic degradation

Enzymatic degradation was carried out under conditions resembling those in the bloodstream (phosphate buffer, pH = 7.4, T = 310 K, 2.5 mmol/L Ca^{2+}) with an amylase activity of 144 units/L. The samples were dissolved in double distilled water (3 % w/w) and poured into the conditioned amylase solution. After a defined time, the enzymatic

degradation was stopped by heating the mixture up to 358 K for five min.

3 Determination of the Chemical Structure

The starch derivatives investigated are the reaction product of an etherification or esterification. The backbone of this class of polymers is starch, a branched polymer consisting of α-(1,4) glycosidic-linked anhydroglucose units (AGU), the chain branchings are formed by α-(1,6) glycosidic bonds. Each AGU has three remaining hydroxyl groups at positions two, three and six, which are available for chemical modification, see Figure 1. The so-called average degree of substitution (DS) is a value representing the total number of substituted hydroxyl functions per AGU. Unsubstituted starch has a DS value of zero and completely substituted starch is identified by a DS of three.

A more detailed description has to differentiate between three possible substitution positions on the AGU: the partial degree of substitution x_i,. The subscript "i" indicates the position two, three or six. The partial degrees of substitution range from zero to one and their sum is the DS.

$$DS = x_2 + x_3 + x_6 \quad (1)$$

The hydroxyethyl substituent enables multiple substitution to take place at one position of the AGU, as shown in Figure 1 for $n > 0$. As a result the production of HES can lead to a most complicated substitution pattern.

The use of quantitatively evaluable carbon NMR spectroscopy leads to the determination of the DS and the three partial degrees of substitution. Figure 2 shows the spectrum of the acetyl starch AS/a 2 (without the carboxyl region). The signal assignment has not yet been published so it was carried out by comparing the spectrum of acetyl starch with another well-known acetyl derivative, the cellulose acetate (similar to the starch derivative, differing only in the glycosidic linkage, β-(1,4) instead of α-(1,4). The chemical shifts of the signals of a cellulose acetate with a DS = 2.0 in Me_2SO-d_6 [9] and of the acetyl starch AS/a 2 are presented in Table 1.

Equation 2 below enables the DS to be determined. The three partial degrees of substitution are calculated with equations 3–5. The determined chemical structure parameters (DS and x_i) of the investigated AS-samples are summarized in Table 2. For comparison a set of HES data from published sources had been added [6].

Tab. 1. ^{13}C-NMR chemical shifts of cellulose acetate referenced against TMS (= 0 ppm) [9] and chemical shifts of acetyl starch referenced against TSP (= – 2.78 ppm) in ppm.

Sample	Cellulose acetate (DS = 2.5) in Me_2SO-d_6	Acetyl starch AS/a 2 in D_2O
C-1 unsubstituted	102.6	102.1
C-1 at 2 substituted	99.6	98.9
C-2, 3, 4, 5	80.2–72.0	79.0–73.6
C-6 substituted	62.6	66.1
C-6 unsubstituted	59.4	62.8
C-7	171.3–170.1	175.6
C-8	20.4/20.1	22.8

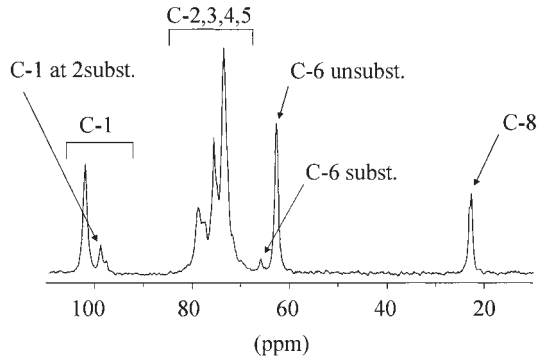

Fig. 2. {^{1}H}-^{13}C-NMR spectrum of the acetyl starch AS/a 2 (DS = 0.5) in deuterium oxide with signal assignments (subst. = substituted; unsubst. = unsubstituted). The region of the carboxyl signal at 175.6 ppm is not shown.

$$DS = \frac{A_{C-8}}{A_{C-1}} \quad (2)$$

$$x_2 = \frac{A_{C-1_{at\,2subst.}}}{A_{C-1}} \quad (3)$$

$$x_6 = \frac{A_{C-6_{subst.}}}{A_{C-6_{subst.+unsubst.}}} \quad (4)$$

$$x_3 = DS - x_2 - x_6 \quad (5)$$

A significant difference in the molecular structure of these two plasma substitutes can be clearly seen. The preferred position for substitution in HES is position two, with the substituent located nearest to the glycosidic linkage. In contrast, position three is preferred in the AS-samples investigated here.

4 Characterization of the Solution Structure

The properties of polymer solutions are influenced by the chemical structure of the polymer chain as well as by the distributions of molar mass and hydrodynamic radius. The mean molar mass is often used to estimate the intravascular retention time in the human circulatory system. However, knowledge of the mean molar mass alone is not sufficient for

Tab. 2. Summary of the chemical structural data of the seven different acetyl starches investigated, the hydroxyethyl starch HES/e 1 and, for comparison, three hydroxyethyl starches taken from the literature [6].

Sample	DS	x_2	x_3	x_6
Acetyl starches				
AS/e 1	0.42	0.17	0.15	0.10
AS/a 2	0.50	0.18	0.27	0.05
AS/e 3	0.58	0.18	0.31	0.09
AS/a 4	0.50	0.16	0.27	0.07
AS/e 5	0.78	0.23	0.42	0.13
AS/a 6	0.81	0.29	0.43	0.09
AS/e 7	0.48	0.21	0.19	0.08
Hydroxyethyl starches				
HES/e 1	0.53	0.28	0.05	0.20
200/0.38	0.34	0.25	0.03	0.06
200/0.47	0.42	0.32	0.04	0.06
200/0.64	0.65	0.42	0.09	0.14

controlling the quality of the product. An acceptable characterization has to include the complete molar mass distribution. Components with low molar mass will be promptly excreted via the kidneys so that the volume effect decreases. High molar mass components are said to give a persistent fraction or to lead to a delayed volume effect [10].

A complete determination of the molar mass distribution is therefore of great interest for the evaluation of these substances. Coupling a fractionation unit, such as size exclusion chromatography (SEC), with a tandem system of a multi-angle laser light-scattering photometer (MALLS), which allows the molar mass to be determined absolutely for each fraction, and a concentration detector (e.g. a differential refractive index detector (DRI)) gives an analytical tool (SEC/MALLS/DRI) for the absolute determination of molar mass distributions. [6, 11].

Formulations of the theory of light scattering were put forward by *Einstein* [12], *Raman* [13], *Debye* [14] and *Zimm* [15], and concise, well-presented summaries of their work can be found in any modern textbook (e.g. reference [16]). MALLS involves measuring the intensity of the scattered light emitted by the sample molecules at different scattering angles, ϑ. For each eluted fraction a molar mass M and a root mean square radius (RMS) can be calculated using the following equations:

$$\frac{Kc}{R_\vartheta} = \frac{1}{P(\vartheta)} \cdot \left(\frac{1}{M} + 2 \cdot A_2 \cdot c + \ldots \right) \qquad (6)$$

and

$$P(\vartheta) = 1 - a_1 \left(2k \sin(\vartheta/2)\right)^2 + a_2 \left(2k \sin(\vartheta/2)\right)^4 - \ldots \qquad (7)$$

where K is a light scattering constant, containing the wavelength λ_o of the incident light, the refractive index n_o of the pure eluent and the refractive index increment dn/dc; c is the concentration, R_ϑ is the excess *Rayleigh* ratio and $P(\vartheta)$ a general form of a scattering function. A_2 is the second virial coefficient. For very low concentrations, the second and higher order terms of equation 6 can usually be neglected. Plotting $Kc/R(\vartheta)$ against $\sin^2(\vartheta/2)$ gives M from the intercept with the ordinate. In addition to this a RMS ($< R_G^2 >^{0.5}$) can be derived from the angular dependence of the intensity of the scattered light, which is included in a_1 and higher order terms of equation 7. For molecules below 10 nm ($\sim \lambda/20$) the precision of the root mean square radius derived from light scattering at λ_0 = 633 nm begins to deteriorate rapidly.

In equation 6 all the constants are given except the refractive index increment, which has to be measured for each polymer solvent pair. All samples were measured in acetate buffer and no evidence was found of the refractive index increment being dependent upon molar mass. On the basis of this results only two samples were measured in sodium nitrate to obtain the corresponding refractive index increment. The results are compiled in Table 3 and used for the calculation of the SEC/MALLS/DRI measurements. Figure 3 shows such a result for an SEC/MALLS/DRI measurement. The polymer concentration is given by the signal of the DRI-detector. In addition to the concentration signal, the corresponding molar masses calculated from the light scattering intensities are also shown. According to the elution mechanism (size exclusion) the molecules with the highest molar mass (and the largest hydrodynamic radius) elute first followed by the smaller ones. Because the light scattering intensity is proportional to the square of the molar mass, the detectability decreases on the "right hand side" of the elution profile, where the smallest molecules elute. The detectable molar masses of the sample AS/a 2 range from $3 \cdot 10^6$ g/mol down to about $6 \cdot 10^3$ g/mol. Weighting the molar mass values with their frequency (concentration signal) gives the absolutely determined molar mass distribution (MMD). Knowing the MMD enables the usual mean values to be calculated. All samples were investigated in 0.1 M $NaNO_3$ solution and in acetate buffer. The values obtained from measurements in acetate buffer were slightly higher than those in 0.1 M $NaNO_3$ solution. The collated values for the acetyl starch samples in Table 3 are the arithmetical mean values of both experimental blocks. Natural starch has molar

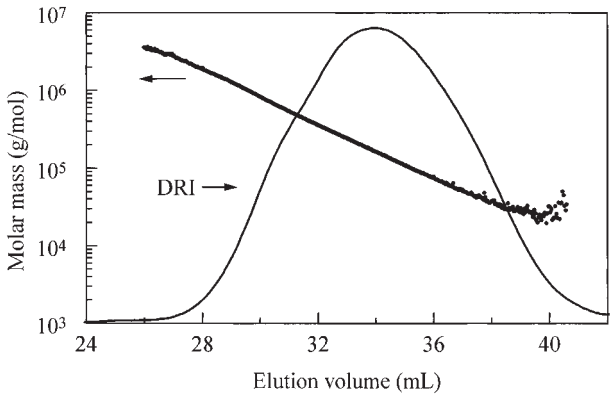

Fig. 3. Elution profile and molar mass obtained by SEC/MALLS/DRI for sample AS/a 2. (T = 298 K, in 0.1 M sodium nitrate solution containing 0.02 % (w/w) sodium azide, λ = 632.8 nm, ϑ = 3°–160°).

Tab. 3. Compilation of the values of refractive index increment in acetate buffer and in 0.1 M $NaNO_3$, molar mass and polydispersity of the investigated acetyl starch samples. The molar mass distributions were measured by SEC/MALLS/DRI.

Sample	dn/dc* (mL/g)	dn/dc** (mL/g)	M_n (g/mol)	M_w (g/mol)	M_z (g/mol)	M_w/M_n (–)	$< R_G^2 >_{z,exp}^{0.5}$ (nm)
AS/e 1	0.135	–	130,000	295,000	660,000	2.4	17
AS/a 2	0.139	–	124,000	302,000	876,000	2.5	18
AS/e 3	0.139	0.133	126,000	288,000	678,000	2.3	17
AS/a 4	0.139	0.133	103,000	252,000	789,000	2.5	18
AS/e 5	0.139	–	126,000	301,000	759,000	2.5	18
AS/a 6	0.135	–	117,000	275,000	773,000	2.4	18
AS/e 7	0.139	–	227,000	766,000	2,619,000	3.6	27

* Refractive index increment in acetate buffer.
** Refractive index increment in 0.1 M $NaNO_3$ – 0.02 % w/w NaN_3.

masses of up to several million; for clinical applications molar masses in the range of ten thousand to one million are needed. In technical applications various different degradation methods are used to obtain starch samples with the "correct" molar masses: for example using enzymatic or ultrasonic degradation, or subjecting the sample to acid hydrolysis. The samples investigated were degraded by enzymes and by acid. From the theoretical point of view two totally different types of distribution might have been obtained. Acid hydrolysis is a random process whereas enzymatic degradation is systematic. But when the cumulative molar mass distributions in Figure 4 were compared, no significant differences in "appearance" and polydispersity were found (see also calculated polydispersities M_w/M_n, Table 3).

As mentioned above, a correct determination of the RMS by MALLS is only possible for the large molecules of the distribution (high molar mass tail), but these values can be used to extrapolate the whole distribution. The results are given in Table 3.

Another way to gain information about the molecular dimensions of the acetyl starch samples is to use the intrinsic viscosity or a hydrodynamic radius of an equivalent sphere for approximation. Equation 8 correlates the mean molar mass with the intrinsic viscosity.

$$[\eta] = k_{[\eta]} M^a \tag{8}$$

Geometric aspects and Equation 8 link the molar mass to a hydrodynamic diameter $d_{eq(\eta)}$

$$d_{eq(\eta)} = \sqrt[3]{\frac{6 \cdot k_{[\eta]} \cdot M^{a+1}}{2.5 \cdot \pi \cdot N_A}} \tag{9}$$

Using the parameters a and $k_{[\eta]}$ for HES in 0.1 M sodium nitrate solution [17] (equation 10) gives representive values for two of the samples included in Table 4.

$$[\eta] = 0.291 \cdot M^{0.35} \tag{10}$$

From the theoretical point of view it is incorrect to use the HES parameters but it can be shown that there is only a slight difference in the solution structure between HES and AS. The calculated $[\eta]$ value can be transformed into a root mean square radius by applying the theory of *Flory* and *Fox* [18] (equations 11–13).

$$< R_G^2 >^{0.5} = k_\nu \cdot M^\nu \tag{11}$$

$$\nu = (a+1)/3 \tag{12}$$

$$k_\nu = \sqrt[3]{k_{[\eta]}/\phi} \tag{13}$$

These data can be compared with RMS values measured during the light scattering experiments. As can be seen in Table 4, there is a good agreement between the measured and the calculated RMS values, which proves the assumption that the solution structures of HES and AS are equivalent.

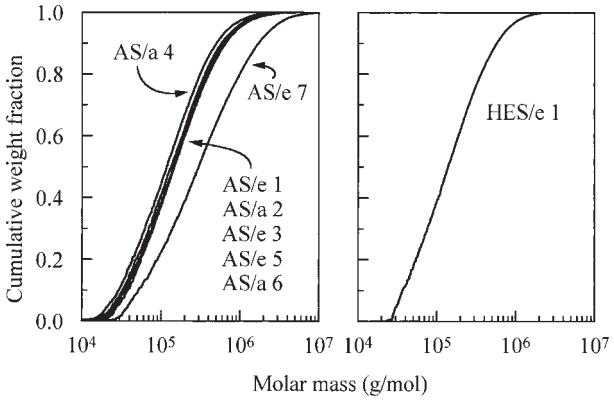

Fig. 4. Cumulative distributions of the molar mass for the AS samples investigated (left) and the hydroxyethyl starch sample investigated, HES/e 1, (right).

5 Enzymatic Degradation

Plasma substitutes should have a defined retention time after which they are completely eliminated. HES is degraded by α-amylase and is excreted via the kidneys.

The degradation behaviour of HES and AS in blood is of fundamental interest. Therefore the sample AS/e 3 and a hydroxyethyl starch sample (HES/e 1) with a comparable molar mass and molar mass distribution (see Figure 4) and a comparable degree of substitution were both treated with α-amylase. The reduction in molar mass was measured by SEC/MALLS/DRI. The results are compiled in Table 5. The alteration of the molar mass distribution of acetyl starch is shown in Figure 5. It can be seen that the width of the molar mass distribution decreases which corresponds to the poly-

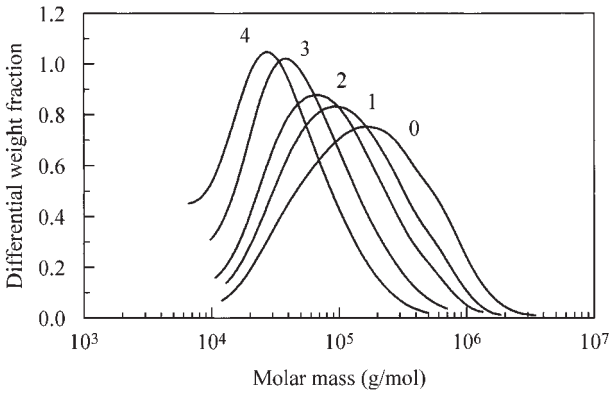

Fig. 5. Enzymatic degradation of the acetyl starch AS/e 3 by α-amylase.
Differential distribution curves determined absolutely by SEC/MALLS/DRI of the non-degraded acetyl starch (0) and after different degradation times (1: 38 min 2: 90 min, 3: 417 min, 4: 1367 min).

Tab. 4. Molecular dimensions of two acetyl starch samples with different molar masses calculated using the theory of *Flory* and *Fox [18]* on the basis of hydroxyethyl starch relationships [17].

Sample	M_w (g/mol)	$[\eta]$ (mL/g)	$d_{eq(\eta)w}$ (nm)	$d_{eq(\eta)z}$ (nm)	$<R_G^2>^{0.5}_{z,calc}$ (nm)	$<R_G^2>^{0.5}_{z,exp}$ (nm)
AS/a 4	252,000	23	19	32	18	18
AS/e 7	766,000	33	32	55	30	27

Tab. 5. Compilation of the molar mass and polydispersity values of the natural and the enzymatically degraded acetyl and hydroxyethyl starch (control) samples (AS/e 3 and HES/e 1). The molar mass distributions were measured by SEC/MALLS/DRI.

Acetyl starch					Hydroxyethyl starch				
time (min)	M_n (g/mol)	M_w (g/mol)	M_z (g/mol)	M_w/M_n (–)	time (min)	M_n (g/mol)	M_w (g/mol)	M_z (g/mol)	M_w/M_n (–)
0	101,000	282,000	709,000	2.8	0	99,000	237,000	540,000	2.4
5	86,000	245,000	548,000	2.8	5	78,000	187,000	407,000	2.4
10	93,000	233,000	512,000	2.5	10	70,000	165,000	337,000	2.4
20	77,000	208,000	506,000	2.7	20	68,000	148,000	300,000	2.2
38	75,000	181,000	413,000	2.4	40	57,000	116,000	230,000	2.0
90	60,000	138,000	324,000	2.3	90	43,000	85,000	173,000	2.0
183	51,000	114,000	259,000	2.2	180	35,000	63,000	115,000	1.8
417	36,000	79,000	167,000	2.2	385	25,000	47,000	87,000	1.9
1367	25,000	50,000	101,000	2.0	1335	17,000	29,000	49,000	1.7

mer becoming more homogeneous. The decrease in molar mass over time is shown in Figure 6. The molar masses at the ordinate were standardized over the measured undegraded molar masses. HES/e 1 and AS/e 3 show an exponential decrease over time. The decrease in the molar mass of acetyl starch is less than that of hydroxyethyl starch.

The degradability of the starch derivatives by α-amylase depends on the degree of substitution. Besides the degree of substitution, the substitution pattern is also a very important factor in degradation by α-amylase. It has been shown for HES that substitution at position C-2 causes a pronounced steric hindrance effect for the α-amylase, whereas this effect is only weak for substitution at position C-6. The C-2/C-6-ratio is therefore a simplified description of the substitution pattern [19], and hence of the biological degradability.

The hydroxyethyl starch sample HES/e 1 has a C-2/C-6-ratio of 1.4. The acetyl starch sample investigated, AS/e 3, has a C-2/C-6-ratio of 2.0. Based on this model of strong and weak hindrance of the substitution at C-2 and C-6, hydroxyethyl starch would thus be expected to undergo faster enzymatic fragmentation.

The sample HES/e 1 is a specially prepared laboratory product. However, when HES/e 1 is compared with the commercially available products (as listed in Table 2), then it can be seen that the latter have a ratio of C-2/C-6 ≅ 4. It may therefore be assumed that the AS (even without any additional cleavage of the substituents by esterase) is broken down in the body better than the customary HES.

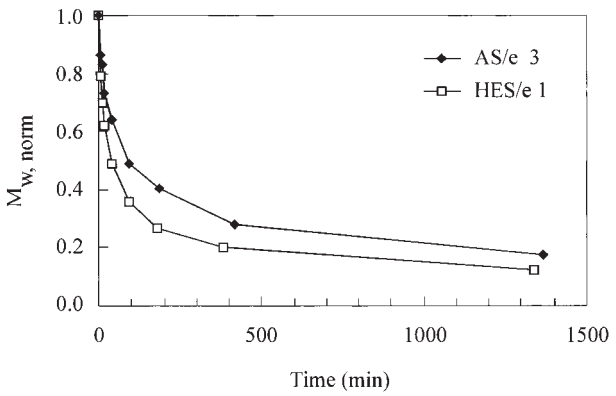

Fig. 6. Enzymatic degradation by α-amylase of the acetyl starch AS/e 3 (rhombus) and the hydroxyethyl starch HES/e 1 (square). Standardised weight-average molar mass: $M_{W,norm} = M_W/M_{W,t=0}$.

6 Symbols and Abbreviations

A_2	second virial coefficient in the *Zimm-Debye*-equation
a	exponent of *Mark-Houwink* ([η]M) equation
a_1, a_2, …	virial coefficients
AGU	anhydroglucose unit
c	concentration
$d_{eq(\eta)}$	hydrodynamic diameter
$d_{eq(\eta)w,z}$	hydrodynamic diameter calculated from $M_{w,z}$
dn/dc	refractive index increment
DRI	differential refractive index
DS	degree of substitution
K	light scattering constant, equal to $\frac{4\pi^2\left(\frac{dn}{dc}\right)^2 n_0^2}{N_A \lambda_0^4}$
$k_{[\eta]\,\nu}$	constant in [η]M-/RM-relationship
k	$2\pi n_0/\lambda_0$
M	molar mass
$M_{n/w/z}$	number/weight/z- average molar mass
MALLS	multi-angle laser light scattering
n_0	refractive index of pure solvent
N_A	*Avogadro* number
$P(\vartheta)$	scattering function
$<R_G^2>_Z^{0.5}$	z-average root mean square radius
R_ϑ	excess *Rayleigh* ratio
RMS	root mean square
x_i	partial degree of substitution

Greek Characters

ϑ	scattering angle
ε	expansion coefficient ($\varepsilon = 2\nu - 1$)
ϕ	*Flory-Fox* constant ($\phi = \phi^0 \cdot (1 - 2.63\varepsilon + 2.86\varepsilon^2)$)
ϕ°	*Flory-Fox* constant for the unperturbed state ($\phi^0 = 3.69 \cdot 10^{24}$ mol^{-1}) [20]
[η]	intrinsic viscosity
ν	exponent of RM equation ($\nu = (a + 1)/3$)
λ_0	vacuum wavelength of incident light

7 Acknowledgements

The samples were kindly provided by Laevosan GmbH, Linz, Austria.

8 Bibliography

[1] *Adams, H. A.*, and *G. Hempelmann:* Therapie mit Volumenersatzmitteln. Anästhesiologie und Intensivmedizin **10** (1991), 277.

[2] *Lutz, H.:* Plasmaersatzmittel. Georg Thieme Verlag, Stuttgart 1975.

[3] Institut für Medizinische Statistik GmbH, Frankfurt 1998.

[4] *Sirtl, C., H. Laubenthal, H. J. Diederich, P. Hügler,* and *K. Peter:* Nebenwirkungen von künstlichen kolloidalen Plasmaersatzmitteln unter besonderer Berücksichtigung von Hydroxyethylstärke (HES). Beitr. Anaesth. Intensivmed. **31** (1990), 35.

[5] *Sommermeyer, K., F. Cech, M. Schmidt,* and *B. Weidler:* Klinisch verwendete Hydroxyethylstärke: Physikalisch-chemische Charakterisierung, Krankenhauspharmazie **8** (1987), 271.

[6] *Kulicke, W.-M., D. Roessner,* and *W. Kull:* Characterization of Hydroxyethyl Starch by Polymer Analysis for Use as a Plasma Volume Expander. Starch/Stärke **45** (1993), 445.

[7] *Förster, H., F. Asskali,* and *E. Nitsch:* Metabolisierbarer Plasmaersatz. Published specification DE 41 22 999 A1, 1993.

[8] *Wyatt, P. J.:* Light scattering and the absolute characterization of macromolecules. Anal. Chim. Acta **272** (1993), 1.

[9] *Doyle, S., R. A. Pethrick, R. K. Harris, J. M. Lane, K. J. Packer,* and *F. Heatley:* ^{13}C nuclear magnetic resonance studies of cellulose acetate in the solution and solid states. Polymer **27** (1986), 19.

[10] *Halmagyi, M.:* Der Einfluß von HES auf die Verteilung von Körperflüssigkeiten, Aktuelle Kongressnachrichten, Innsbruck 3./4. April 1992.

[11] *Jackson, C., L. M. Nilsson,* and *P. J. Wyatt:* Characterization of Biopolymers using a Multi-Angle Light Scattering Detector with Size Exclusion Chromatography. J. Appl. Polym. Sci. **43** (1989), 99.

[12] *Einstein, A.:* Theorie der Opaleszenz von homogenen Flüssigkeiten in der Nähe des kritischen Zustandes. Ann. Phys. **33** (1910), 1275.

[13] *Raman, C. V.:* Relation of Tyndall Effect to Osmotic Pressure in Colloidal Solutions, Indian J. Phys. **2** (1927), 1.

[14] *Debye, P.:* Light Scattering in Solutions, J. Appl. Phys. **15** (1944), 338.

[15] *Zimm, B. H.:* Molecular Theory of the Scattering of Light in Fluids. J. Chem. Phys. **13** (1945), 141.

[16] *Kratochvil, P.:* Classical Light Scattering from Polymer Solutions. Jenkins A. D. (Ed.), Amsterdam, Elsevier 1987.

[17] *Granath, K. A., R. Strömberg,* and *A. N. de Belder:* Studies on hydroxyethyl starch. Fractionation and molecular weight distribution by gel chromatography. Starch/Stärke **21** (1969), 251.

[18] *Flory, P. J.,* and *T. G. Fox:* Treatment of Intrinsic Viscosities. J. Am. Chem. Soc. **73** (1951), 1904.

[19] *Yoshida, M., Y. Muiami,* and *T. Kishikawa:* A Study of Hydroxyethyl Starch Part III. Comparison of Metabolic Fates between 2-O-Hydroxyethyl Starch and 6-O-Hydroxyethyl Starch in Rabbits. Starch/Stärke **36** (1984), 209.

[20] *Yamakawa, H.:* Modern Theory of Polymer Solutions. New York, Harper and Row, 1971.

Address of authors: Dipl.-Chem. *Dorothee Heins,* Prof. Dr.-Ing. *Werner-Michael Kulicke,* Dr. *Peter Käuper,* and Dr. *Heiko Thielking.* Universität Hamburg, Institut für Technische und Makromolekulare Chemie. D-20146 Hamburg (Germany).

(Received: May 25, 1998).